Antiproton Low - Energy Collisions with Ps-atoms & True Muonium Atoms

Renat A. Sultanov

St. Cloud State University, St. Cloud, MN, USA

11-th International LEAP Conference, Uppsala, Sweden

Tuesday, June 11, 2013

ABSTRACT

- A few-body type computation: 3-charge-particle collision with participation of a slow antiproton and Ps and a muonic muonium atom (True Muonium):

$$\bar{\mathrm{p}} + (e^+e^-)_{1s} \to \overline{\mathrm{H}} + e^-,$$

$$\bar{\mathrm{p}} + (\mu^+\mu^-)_{1s} \to \overline{\mathrm{H}}_\mu + \mu^-.$$

- 3-body Coulomb system.
- Instead of 3 coupled Faddeev equations, just 2 coupled **Faddeev-Hahn-type** equations are used.
- Solution: a modified close coupling expansion approach and K-matrix method.

TWO SPATIAL CONFIGURATIONS

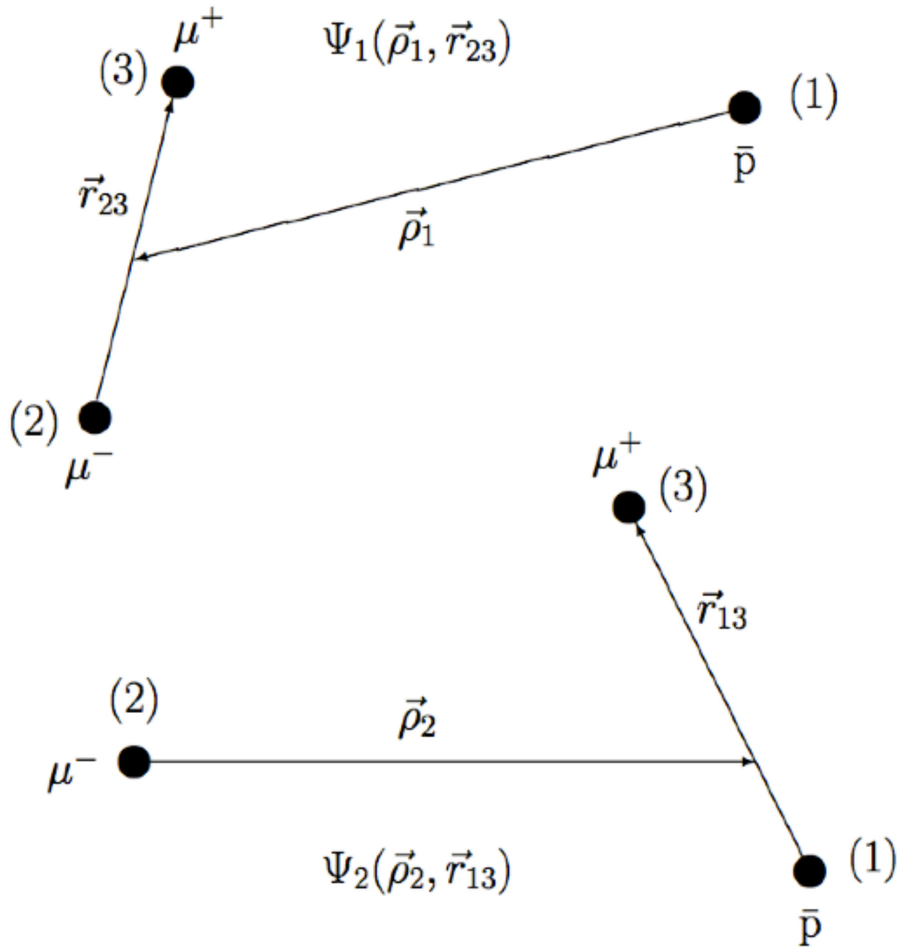

CONFIGURATION TRIANGLE (123)

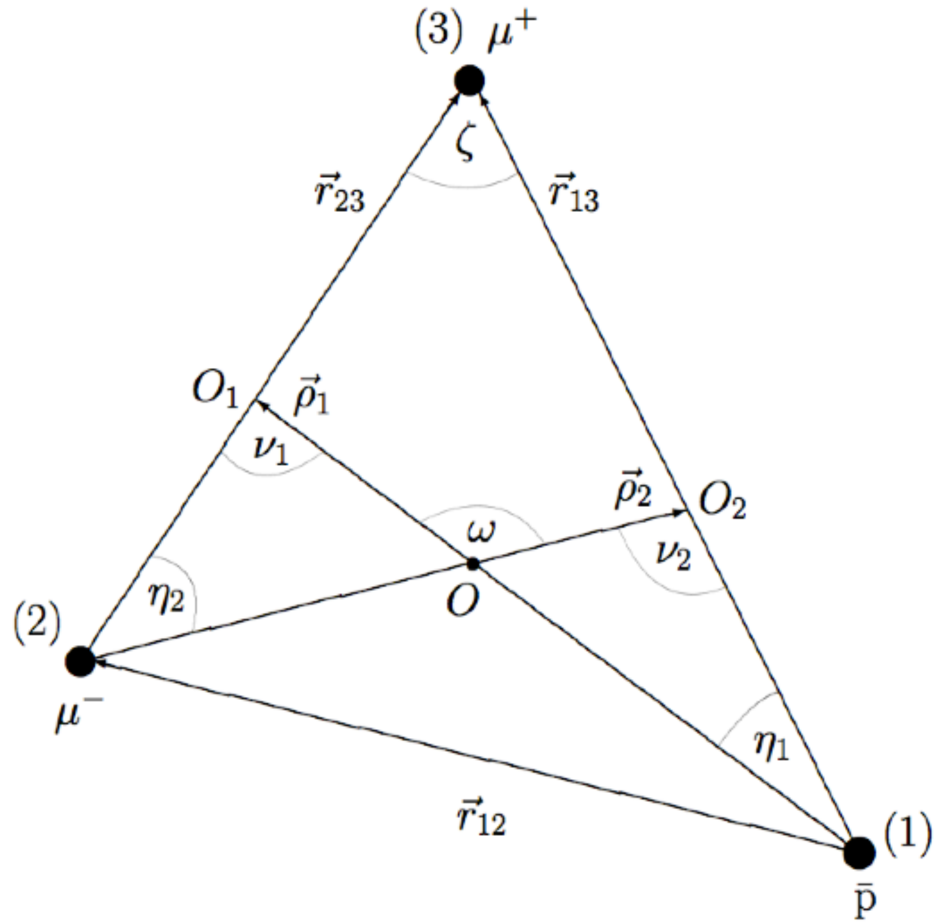

outline

1. WHY ANTIMATTER?
2. Recent developments & **experiments:** ATRAP, ASACUSA, ALPHA … ***CERN***
3. Anti-hydrogen, muonic antihydrogen, Ps atoms, slow antiprotons etc.
4. **Theory:** 3- and 4-body Coulombic quantum systems. Collisions, bound states, resonances(?) etc.
5. **Faddeev, AGS and Faddeev-Hahn-type equations.**
6. Numerical approach: discretization and matrix method.
7. Results and conclusions.

WHY ANTIMATTER?

- GOALS: TO PRODUCE COLD $\bar{H}$; TO TRAP COLD $\bar{H}$; TO COMPARE H and $\bar{H}$ WITH THE USE OF LASER SPECTR-OSCOPY.
- CPT SYMMETRY: Particles and anti-particles have same mass, same mean life, same magnetic moment, and… opposite charge!
- ATOM and ANTI-ATOM HAVE SAME STRUCTURE?

WHY H and $\bar{H}$?

- Spectroscopic measurement on **$\bar{H}$** in comparison with corresponding results for normal **H**.
- This comparison may contribute to the verification OR falsification of the CPT conservation law.
- Gravitational measurements of $\bar{H}$ and H and .....
- Antimatter may even be related to the **dark matter** problem in astrophysics.

LOW ENERGY ANTIPROTON (**pbar** = p^- = $\overline{p}$) and $\overline{H}$ PHYSICS

- Collision experiments with antiprotons: H_2 ionization with **pbar**: significant deviation between experimental results and theory.
- Antiprotonic helium experiments: CPT & fundamental constants. Temp. $T < 1$ K!
- **pbar** + He^+ experiments and theory: pbar+$^4He^+$ and pbar+$^3He^+$ - ATOMCULE!

at ASACUSA TEAM **(RIKEN, JAPAN)**.

ASACUSA = *ATOMIC*
SPECTROSCOPY
AND
COLLISIONS
USING
SLOW ANTIPROTONS

ATRAP = *ANTIHYDROGEN TRAP*

ALPHA = *Antihydrogen Laser Physics Apparatus*

<u>ATHENA</u> = *ANTIHYDROGEN PRODUCTION AND PRECISION EXPERIMENTS*

========================

In 2002, it was the first experiment to produce 50,000 low-energy $\bar{\mathbf{H}}$**.**

<u>Nature 419, 456 (2002).</u>

MUON PHYSICS: H_μ and $\bar{H}_\mu$ EVEN BETTER ?

- In book: "Introductory Muon Science", 2003:

  K. Nagamine pointed out: muonic antihydrogen atom might be even better choice to check the CPT law than usual antihydrogen atom, i.e. $\bar{H}$.

- Therefore there is a significant need to know the formation rates of $\bar{H}_\mu$ atoms at low and very low energies from ~ 5eV down to ~ 10^{-3} eV.

"If the CPT violating interaction is short range with an extremely massive exchange boson such an effect can be detected more easily in the case of muonic antihydrogen than in simple antihydrogen. This is because the size of the $\bar{\mathbf{H}}_{\mu}$ atom is ~207 times smaller than $\bar{\mathbf{H}}$".

FEW-BODY REACTIONS for H̄ and H̄$_\mu$ FORMATION (1)-(5)

$$\bar{\mathrm{p}} + \mathrm{Ps} \rightarrow \bar{\mathrm{H}} + e^- \tag{1}$$

$$\bar{\mathrm{p}} + (\mathrm{Ps})_\mu \rightarrow \bar{\mathrm{H}}_\mu + \mu^- \tag{2}$$

$$\bar{\mathrm{p}} + \mathrm{Mu} \rightarrow \bar{\mathrm{H}}_\mu + e^- \tag{3}$$

$$\bar{\mathrm{p}} + e^+ + e^+ \rightarrow \bar{\mathrm{H}} + e^+ \tag{4}$$

$$\bar{\mathrm{p}} + \mu^+ + \mu^+ \rightarrow \bar{\mathrm{H}}_\mu + \mu^+ \tag{5}$$

MUON TRANSFER 3-BODY REACTIONS (6)-(8) of MUON CATALYZED FUSION CYCLE (μCF - cycle)

$$t^+ + (d^+\mu^-)_{1s} \rightarrow (t^+\mu^-)_{1s} + d^+ \qquad (6)$$

$$t^+ + (p^+\mu^-)_{1s} \rightarrow (t^+\mu^-)_{1s} + p^+ \qquad (7)$$

$$d^+ + (p^+\mu^-)_{1s} \rightarrow (d^+\mu^-)_{1s} + p^+ \qquad (8)$$

Only 2 [*not 3!*] asymptotic-spatial configuration subsystems

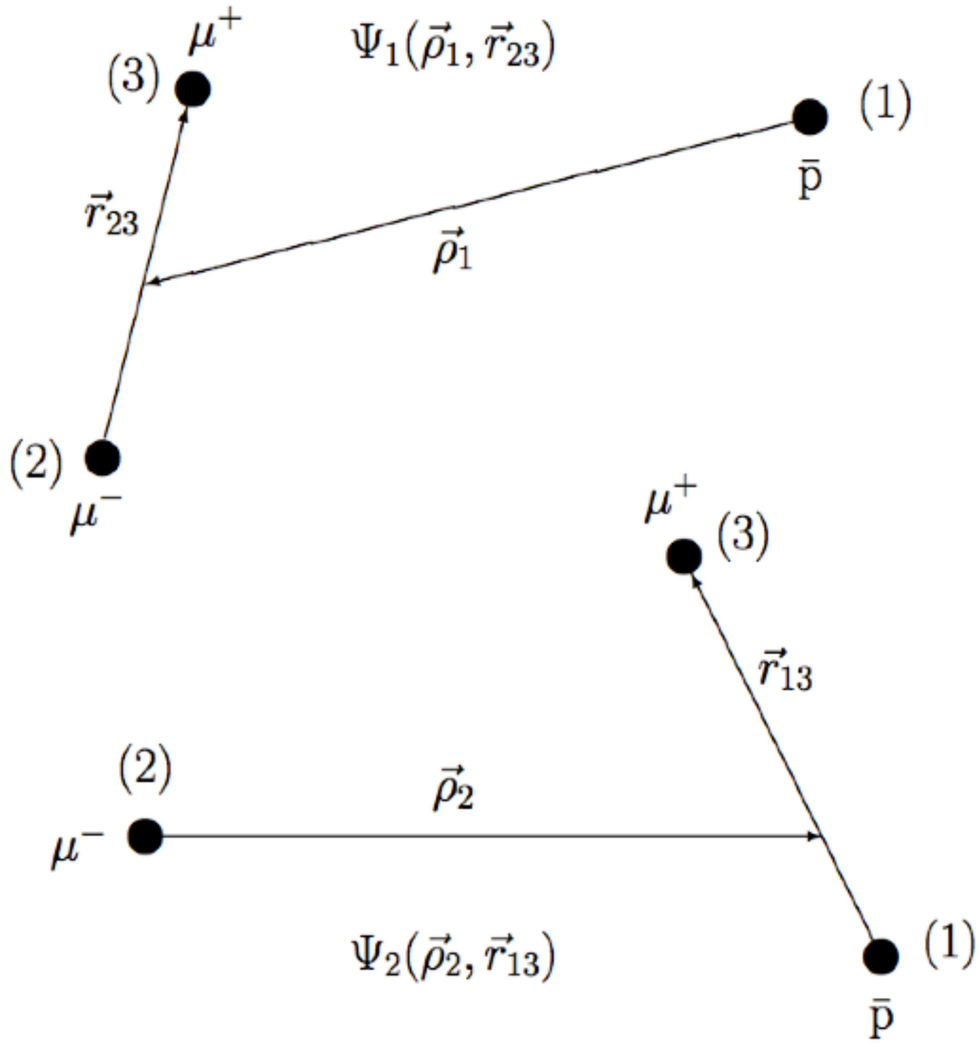

JACOBI COORDINATES, MASSES and EQUATIONS

3-body systems with **arbitrary** masses & the 3-body W.F. is represented as:

$$\vec{r}_{j3} = \vec{r}_3 - \vec{r}_j,$$

$$\vec{\rho}_k = (\vec{r}_3 + m_j \vec{r}_j)/(1 + m_j) - \vec{r}_k, \quad (j \neq k = 1, 2).$$

$$|\Psi\rangle = \Psi_1(\vec{r}_{23}, \vec{\rho}_1) + \Psi_2(\vec{r}_{13}, \vec{\rho}_2),$$

$$\overline{\mathrm{p}} + (\mu^+ \mu^-)_{1s} \rightarrow \overline{\mathrm{H}}_\mu + \mu^-.$$

FADDEEV-HAHN-type EQUATIONS

- A set of **two** coupled equations:

$$\left(E-\hat{H}_0-V_{23}(\vec{r}_{23})\right)\Psi_1(\vec{r}_{23},\vec{\rho}_1)=\left(V_{23}(\vec{r}_{23})+V_{12}(\vec{r}_{12})\right)\Psi_2(\vec{r}_{13},\vec{\rho}_2),$$

$$\left(E-\hat{H}_0-V_{13}(\vec{r}_{13})\right)\Psi_2(\vec{r}_{13},\vec{\rho}_2)=\left(V_{13}(\vec{r}_{13})+V_{12}(\vec{r}_{12})\right)\Psi_1(\vec{r}_{23},\vec{\rho}_1).$$

1) The constructed coupled equations satisfy the Schrödinger Eq. exactly.
2) The Faddeev decomposition avoids the overcompleteness problems.

3) Two-body subsystems are treated in an equivalent way AND the correct asymptotics are guaranteed.

4) It simplifies the solution procedure and provides the correct asymptotic behavior of the solution below the 3-body break-up threshold.

5) FH equations have the same advantages as the Faddeev equations, because they are formulated for the w.f. components with correct physical asymptotes: **Y. Hahn, Phys. Rev. 169, 794 (1968).**

ASYMPTOTICS

for only two components:

$$\Psi_1(\vec{r}_{23},\vec{\rho}_1) \underset{\rho_1\to+\infty}{\sim} e^{ik_1 z}\varphi_1(\vec{r}_{23}) + \sum_n^{\infty} A_n^{el/ex}(\Omega_{\rho_1})\frac{e^{ik_n\rho_1}}{\rho_1}\varphi_n(\vec{r}_{23}),$$

$$\Psi_2(\vec{r}_{13},\vec{\rho}_2) \underset{\rho_2\to+\infty}{\sim} \sum_m^{\infty} A_m^{tr}(\Omega_{\rho_2})\frac{e^{ik'_m\rho_2}}{\rho_2}\varphi_m(\vec{r}_{13}).$$

$$\mathrm{Li}^{3+} + (\mathrm{p}^{+}\mu^{-})_{1\mathrm{s}} \rightarrow (\mathrm{Li}_{\mu}^{2+})_{1\mathrm{s}} + \mathrm{p}^{+}.$$

$$\left(E - \hat{h}_{23}(\vec{r}_{23}) - \hat{T}_1(\vec{\rho}_1)\right)\Psi_1(\vec{r}_{23},\vec{\rho}_1) = \left(V_{23}(\vec{r}_{23}) + V_{12}(\vec{r}_{12}) - \frac{(Z_1-1)Z_2}{\rho_2}\right)\Psi_2^C(\vec{r}_{13},\vec{\rho}_2),$$

$$\left(E - \hat{h}_{13}(\vec{r}_{13}) - \hat{T}_2(\vec{\rho}_2) - \frac{(Z_1-1)Z_2}{\rho_2}\right)\Psi_2^C(\vec{r}_{13},\vec{\rho}_2) = \left(V_{13}(\vec{r}_{13}) + V_{12}(\vec{r}_{12})\right)\Psi_1(\vec{r}_{23},\vec{\rho}_1).$$

$$\Psi_1(\vec{r}_{23},\vec{\rho}_1) \underset{\rho_1\to+\infty}{\sim} e^{ik_1^{(1)}z}\varphi_1(\vec{r}_{23}) + \sum_n A_n^{\mathrm{el/in}}(\Omega_{\rho_1})\frac{e^{ik_n^{(1)}\rho_1}}{\rho_1}\varphi_n(\vec{r}_{23}),$$

$$\Psi_2^C(\vec{r}_{13},\vec{\rho}_2) \underset{\rho_2\to+\infty}{\sim} \sum_{ml} A_{ml}^{\mathrm{tr}}(\Omega_{\rho_2})\frac{e^{i(k_m^{(2)}\rho_2 - \pi l/2 + \tau_l - \eta/2k_m^{(2)}\ln 2k_m^{(2)}\rho_2)}}{\rho_2}\varphi_m(\vec{r}_{13}).$$

$$\left(E + \frac{1}{2M_k}\Delta_{\vec{\rho}_k} + \frac{1}{2\mu_j}\Delta_{\vec{r}_{j3}} - V_{j3}\right)\Psi_i(\vec{r}_{j3}, \vec{\rho}_k) = \left(V_{j3} + V_{jk}\right)\Psi_{i'}(\vec{r}_{k3}, \vec{\rho}_j\right), \qquad (17)$$

here $i \neq i' = 1, 2$, $M_k^{-1} = m_k^{-1} + (1+m_j)^{-1}$ and $\mu_j^{-1} = 1 + m_j^{-1}$. In order to separate angular variables, the wave function components Ψ_i are expanded over bipolar harmonics:

$$\{Y_\lambda(\hat{\rho}) \otimes Y_l(\hat{r})\}_{LM} = \sum_{\mu m} C^{LM}_{\lambda\mu l m} Y_{\lambda\mu}(\hat{\rho}) Y_{lm}(\hat{r}), \qquad (18)$$

$$\Psi_i(\vec{r}_{j3}, \vec{\rho}_k) = \sum_{LM\lambda l} \Phi^i_{LM\lambda l}(\rho_k, r_{j3}) \left\{Y_\lambda(\hat{\rho}_k) \otimes Y_l(\hat{r}_{j3})\right\}_{LM} \qquad (19)$$

$$\Phi^i_{LM\lambda l}(\rho_k, r_{j3}) = \frac{1}{\rho_k} \sum_n f^{(i)LM}_{nl\lambda}(\rho_k) R^{(i)}_{nl}(r_{j3}),$$

$$2M_k(E - E^i_n) f^i_\alpha(\rho_k) + \left(\frac{\partial^2}{\partial\rho_k^2} - \frac{\lambda(\lambda+1)}{\rho_k^2}\right) f^i_\alpha(\rho_k) = \frac{M_k}{\gamma^{-3}} \sum_{\alpha'} \int_0^\infty d\rho_j S^{ii'}_{\alpha\alpha'}(\rho_j, \rho_k) f^{i'}_{\alpha'}(\rho_j),$$

$$S^{ii'}_{\alpha\alpha'}(\rho_j, \rho_k) = 2\rho_j\rho_k \int d\hat{\rho}_j \int d\hat{\rho}_k R^i_{nl}(r_{j3}) \left\{Y_\lambda(\hat{\rho}_k) \otimes Y_l(\hat{r}_{j3})\right\}^*_{LM} \left(V_{j3} + V_{jk}\right)$$
$$\left\{Y_{\lambda'}(\hat{\rho}_j) \otimes Y_{l'}(\hat{r}_{k3})\right\}_{LM} R^{i'}_{n'l'}(r_{k3}) \, .$$

$$\vec{\rho}_j = \vec{r}_{j3} - \beta_k \vec{r}_{k3}, \quad \vec{r}_{j3} = \frac{1}{\gamma}(\beta_k \vec{\rho}_k + \vec{\rho}_j), \quad \vec{r}_{jk} = \frac{1}{\gamma}(\sigma_j \vec{\rho}_j - \sigma_k \vec{\rho}_k),$$

$$\beta_k = m_k/(1+m_k), \quad \sigma_k = 1 - \beta_k, \quad \gamma = 1 - \beta_k\beta_j \quad (j \neq k = 1,2),$$

$$\left((k_n^i)^2 + \frac{\partial^2}{\partial\rho_i^2} - \frac{\lambda(\lambda+1)}{\rho_i^2}\right) f_\alpha^i(\rho_i) = g \sum_{\alpha'} \sqrt{\frac{(2\lambda+1)(2\lambda'+1)}{(2L+1)}} \int_0^\infty d\rho_{i'} f_{\alpha'}^{i'}(\rho_{i'})$$

$$\int_0^\pi d\omega \sin\omega R_{nl}^i(r_{i'3}) \Big(V_{i'3}(r_{i'3}) + V_{ii'}(r_{ii'})\Big) R_{n'l'}^{i'}(r_{i3}) \rho_{i'} \rho_i$$

$$\sum_{mm'} D_{mm'}^L(0,\omega,0) C_{\lambda 0 lm}^{Lm} C_{\lambda' 0 l' m'}^{Lm'} Y_{lm}(\nu_i, \pi) Y_{l'm'}^*(\nu_{i'}, \pi). \qquad (32)$$

For the sake of simplicity $\alpha \equiv (nl\lambda)$ are quantum numbers of a three-body state and L is the total angular momentum of the three-body system, $g = 4\pi M_i/\gamma^3$, $k_n^i = \sqrt{2M_i(E - E_n^{i'})}$, where $E_n^{i'}$ is the binding energy of the subsystem $(i'3)$, $M_1 = m_1(m_2+m_3)/(m_1+m_2+m_3)$ and $M_2 = m_2(m_1+m_3)/(m_1+m_2+m_3)$ are the reduced masses, $\gamma = 1 - m_i m_{i'}/((m_i + 1)(m_{i'}+1))$, $D_{mm'}^L(0,\omega,0)$ the Wigner functions, $C_{\lambda 0 lm}^{Lm}$ the Clebsh-Gordon coefficients, Y_{lm} are the spherical functions, ω is the angle between the Jacobi coordinates $\vec{\rho}_i$ and $\vec{\rho}_{i'}$, ν_i is the angle between $\vec{r}_{i'3}$ and $\vec{\rho}_i$, $\nu_{i'}$ is the angle between $\vec{r}_{i3}$ and $\vec{\rho}_{i'}$. One can show that: $\sin\nu_i = (\rho_k r_{kj})/\gamma \sin\omega$, and $\cos\nu_i = (\beta\rho_i + \rho_k \cos\omega)/(\gamma r_{kj})$.

Vectors & Angles of the 3-Body System (123)

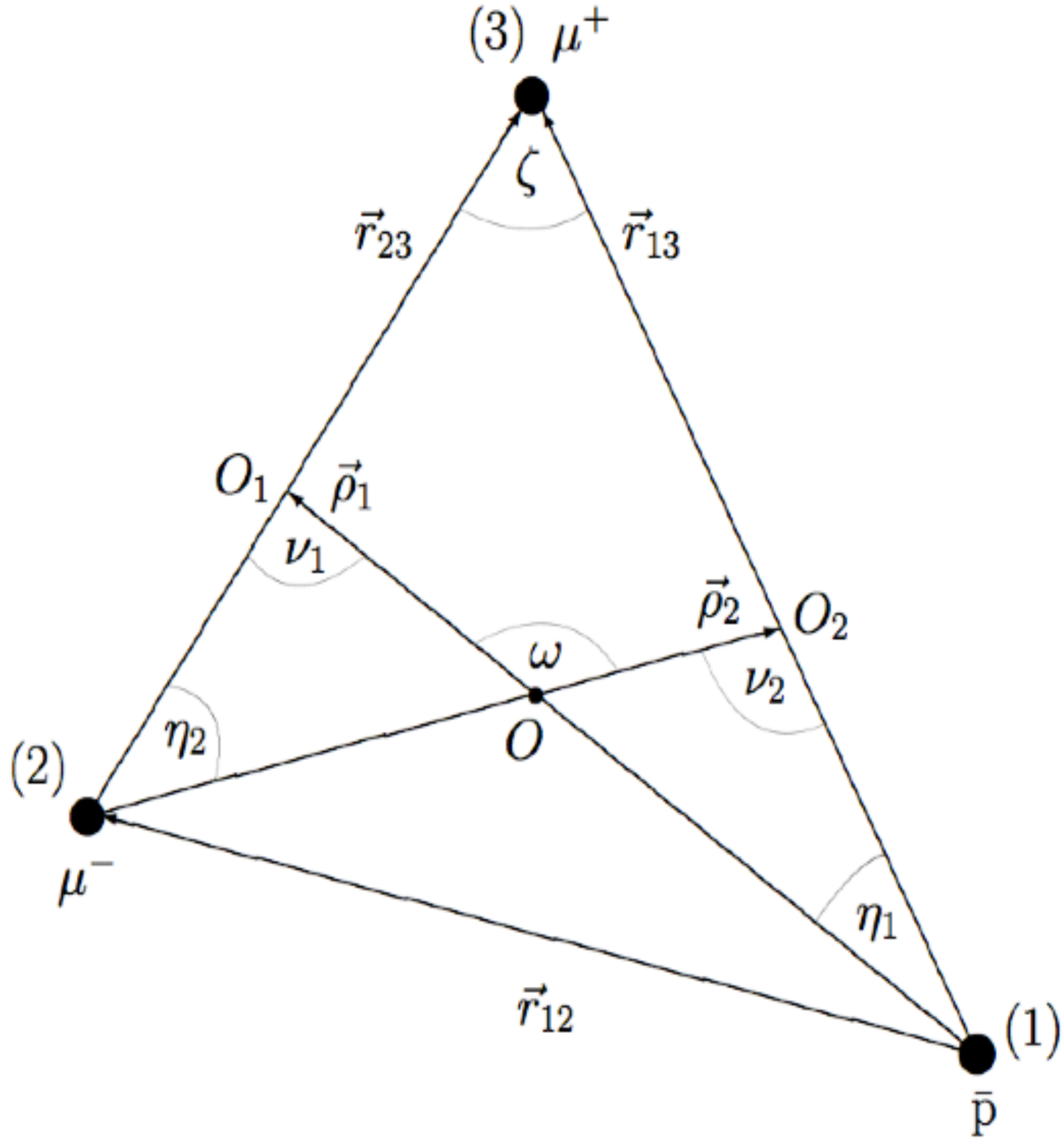

K-matrix formalism:

$K_{12} = K_{21}$ or $K_{12} / K_{21} = 1.0$!

arXiv:1304.2434v2

$$\begin{cases} f_{1s}^{(i)}(\rho_i) \underset{\rho_1 \to +\infty}{\sim} \sin(k_1^{(i)}\rho_i) + K_{ii}\cos(k_1^{(i)}\rho_i) \\ f_{1s}^{(j)}(\rho_j) \underset{\rho_j \to +\infty}{\sim} \sqrt{v_i/v_j} K_{ij}\cos(k_1^{(j)}\rho_j) \,, \end{cases}$$

$$\sigma_{ij} = \frac{4\pi}{k_1^{(i)2}} \left| \frac{\mathbf{K}}{1 - i\mathbf{K}} \right|^2 = \frac{4\pi}{k_1^{(i)2}} \frac{\delta_{ij} D^2 + K_{ij}^2}{(D-1)^2 + (K_{11} + K_{22})^2},$$

Discretization Procedure:
J. Comp. Phys. 192, 231-243 (2003)

$$\left[k_n^{(1)2} + D_{ij}^2 - \frac{\lambda(\lambda+1)}{\rho_{1i}^2}\right] f_\alpha^{(1)}(i) \; - \; \frac{M_1}{\gamma^3} \sum_{\alpha'=1}^{N_s} \sum_{j=1}^{N_p} w_j S_{\alpha\alpha'}^{(12)}(\rho_{1i}, \rho_{2j}) f_{\alpha'}^{(2)}(j) = 0,$$

$$-\frac{M_2}{\gamma^3} \sum_{\alpha=1}^{N_s} \sum_{j=1}^{N_p} w_j S_{\alpha'\alpha}^{(21)}(\rho_{2i}, \rho_{1j}) f_\alpha^{(1)}(j) \; + \; \left[k_{n'}^{(2)2} + D_{ij}^2 - \frac{\lambda'(\lambda'+1)}{\rho_{2i}^2}\right] f_{\alpha'}^{(2)}(i) = B_{\alpha'}^{21}(i).$$

$$D_{ij}^2 f_\alpha(i) = (f_\alpha(i-1)\delta_{i-1,j} - 2 f_\alpha(i)\delta_{i,j} + f_\alpha(i+1)\delta_{i+1,j})/\Delta,$$

$$B_{\alpha'}^{(21)}(i) \; = \; M_2/\gamma^3 \sum_{j=1}^{N_p} w_j S_{\alpha' 1 s 0}^{(21)}(i,j) \sin(k_1 \rho_j),$$

	1s′	2s′	2p′	1s	2s	2p	
1s	$\ddots$	**A**=0...	0...	$-\frac{M_1}{\gamma^3} S^{(12)}_{1s:1s'}$	$-\frac{M_1}{\gamma^3} S^{(12)}_{1s:2s'}$	$-\frac{M_1}{\gamma^3} S^{(12)}_{1s:2p'}$	
2s	0...	$\ddots$	0...	$-\frac{M_1}{\gamma^3} S^{(12)}_{2s:1s'}$	$-\frac{M_1}{\gamma^3} S^{(12)}_{2s:2s'}$	$-\frac{M_1}{\gamma^3} S^{(12)}_{2s:2p'}$	
2p	0...	0...	$\ddots$	$-\frac{M_1}{\gamma^3} S^{(12)}_{2p:1s'}$	$-\frac{M_1}{\gamma^3} S^{(12)}_{2p:2s'}$	$-\frac{M_1}{\gamma^3} S^{(12)}_{2p:2p'}$	
	$-\frac{M_2}{\gamma^3} S^{(21)}_{1s':1s}$	$-\frac{M_2}{\gamma^3} S^{(21)}_{1s':2s}$	$-\frac{M_2}{\gamma^3} S^{(21)}_{1s':2p}$	$\ddots$	**A**=0...	0...	1s′
	$-\frac{M_2}{\gamma^3} S^{(21)}_{2s':1s}$	$-\frac{M_2}{\gamma^3} S^{(21)}_{2s':2s}$	$-\frac{M_2}{\gamma^3} S^{(21)}_{2s':2p}$	0...	$\ddots$	0...	2s′
	$-\frac{M_2}{\gamma^3} S^{(21)}_{2p':1s}$	$-\frac{M_2}{\gamma^3} S^{(21)}_{2p':2s}$	$-\frac{M_2}{\gamma^3} S^{(21)}_{2p':2p}$	0...	0...	$\ddots$	2p′

$$\sum_{\alpha'=1}^{2\times N_s} \sum_{j=1}^{N_p} \mathbf{A}_{\alpha\alpha'}(i,j)\vec{f}_{\alpha'}(j) = \vec{b}_{\alpha}(i).$$

$$S_{\alpha\alpha'}^{(ii')}(\rho_i,\rho_{i'}) = \frac{4\pi}{\beta_i}\frac{[(2\lambda+1)(2\lambda'+1)]^{\frac{1}{2}}}{2L+1}\int_{|\beta_i\rho_i-\rho_{i'}|}^{\beta_i\rho_i+\rho_{i'}} dx R_{nl}^{(i)}(x)\left[-1+\frac{x}{r_{ii'}(x)}\right] R_{n'l'}^{(i')}(r_{i3}(x))$$
$$\sum_{mm'} D_{mm'}^{L}(0,\omega(x),0)C_{\lambda 0 lm}^{Lm}C_{\lambda' 0 l'm'}^{Lm'}Y_{lm}(\nu_i(x),\pi)Y_{l'm'}^{*}(\nu_{i'}(x),\pi). \quad (40)$$

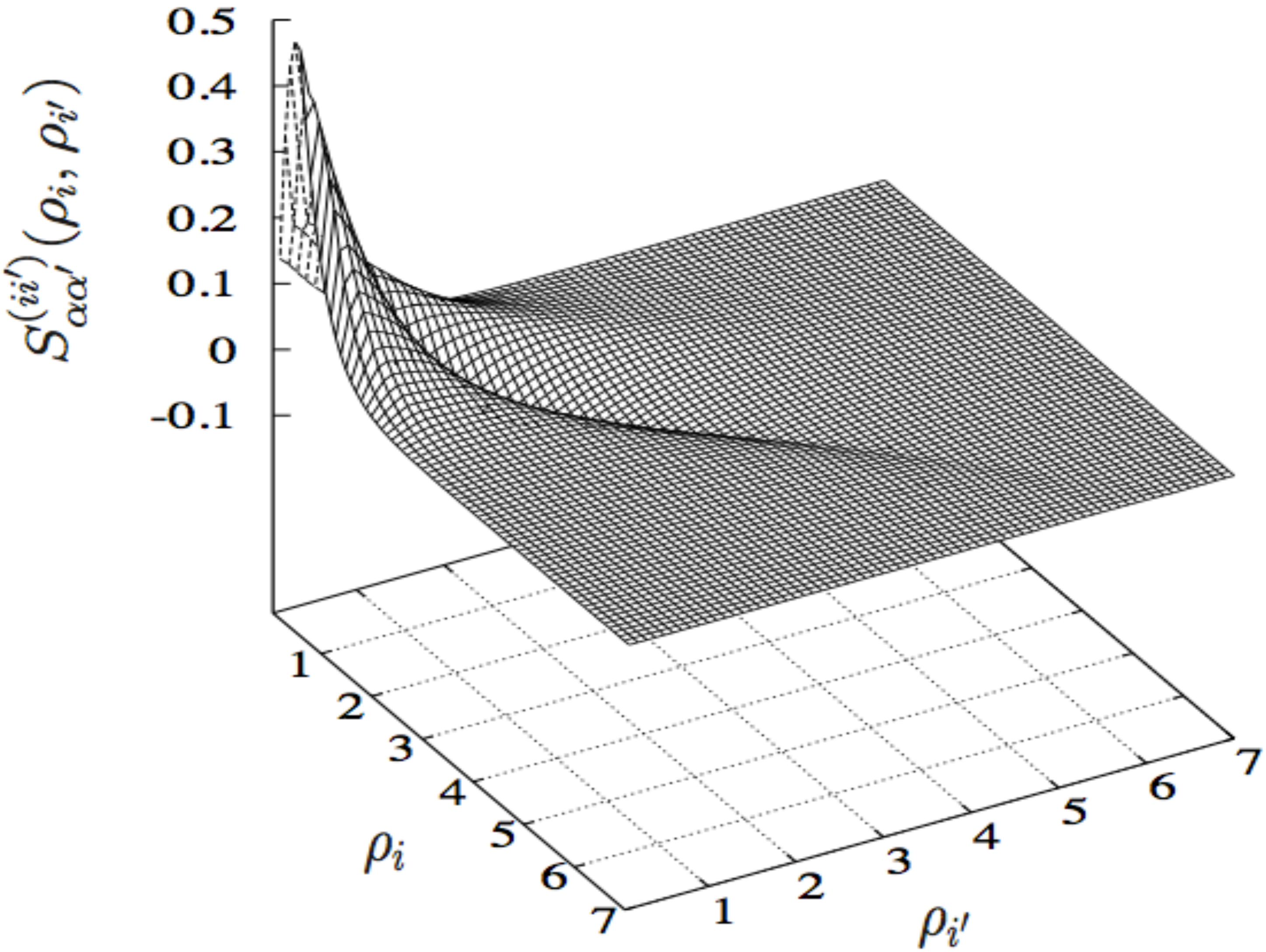

FIG. 3. The angular integral $S^{ii'}_{\alpha\alpha'}(\rho_i, \rho_{i'})$, Eq. (40), in the input channel $\overline{\mathrm{p}} + (\mu^+\mu^-)$ when $\alpha =$1s and $\alpha' =$1s.

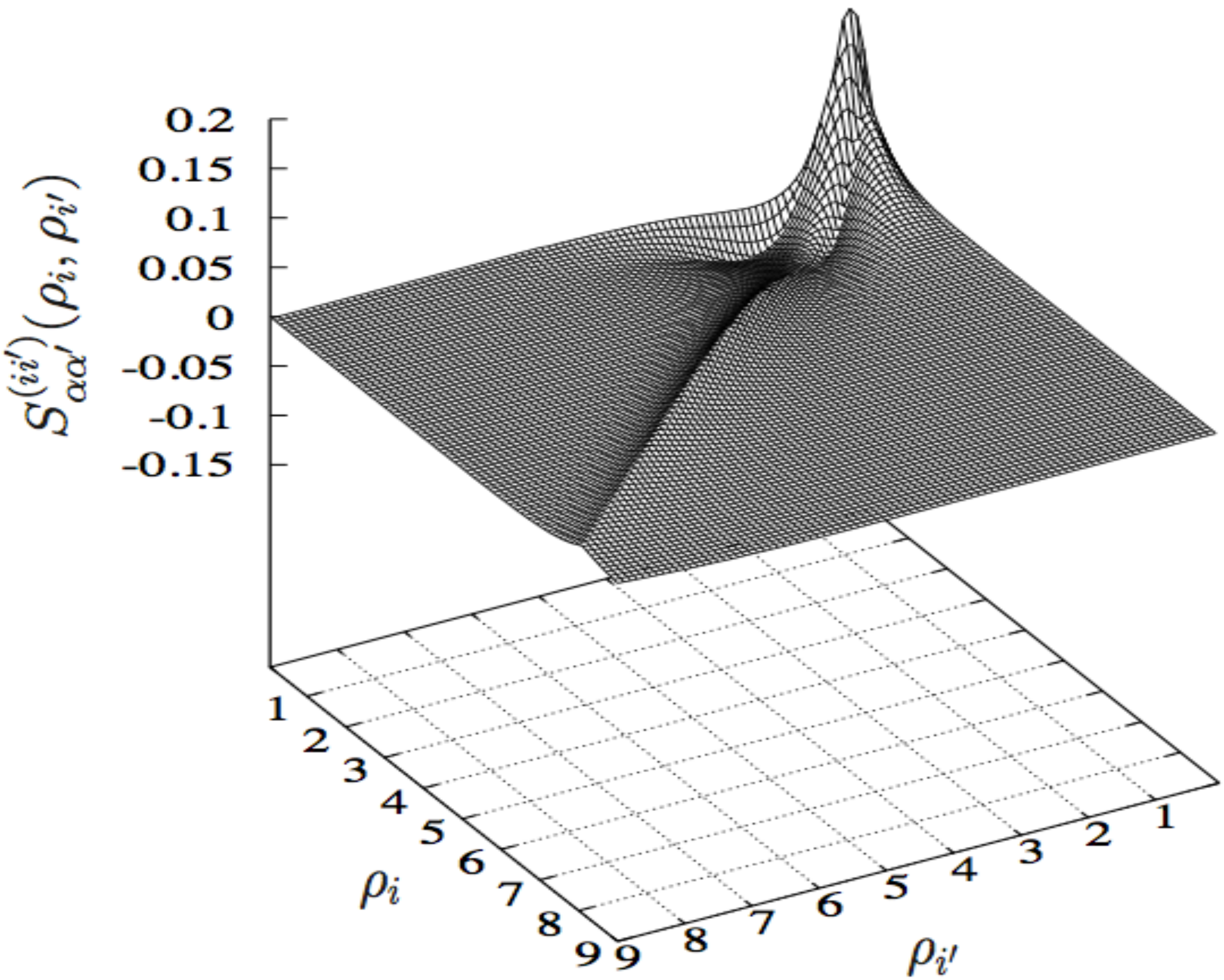

FIG. 4. The angular integral $S_{\alpha\alpha'}^{ii'}(\rho_i, \rho_{i'})$, Eq. (40), in the input channel $\overline{\mathrm{p}} + (\mu^+\mu^-)$ when α =1s and α' =2s.

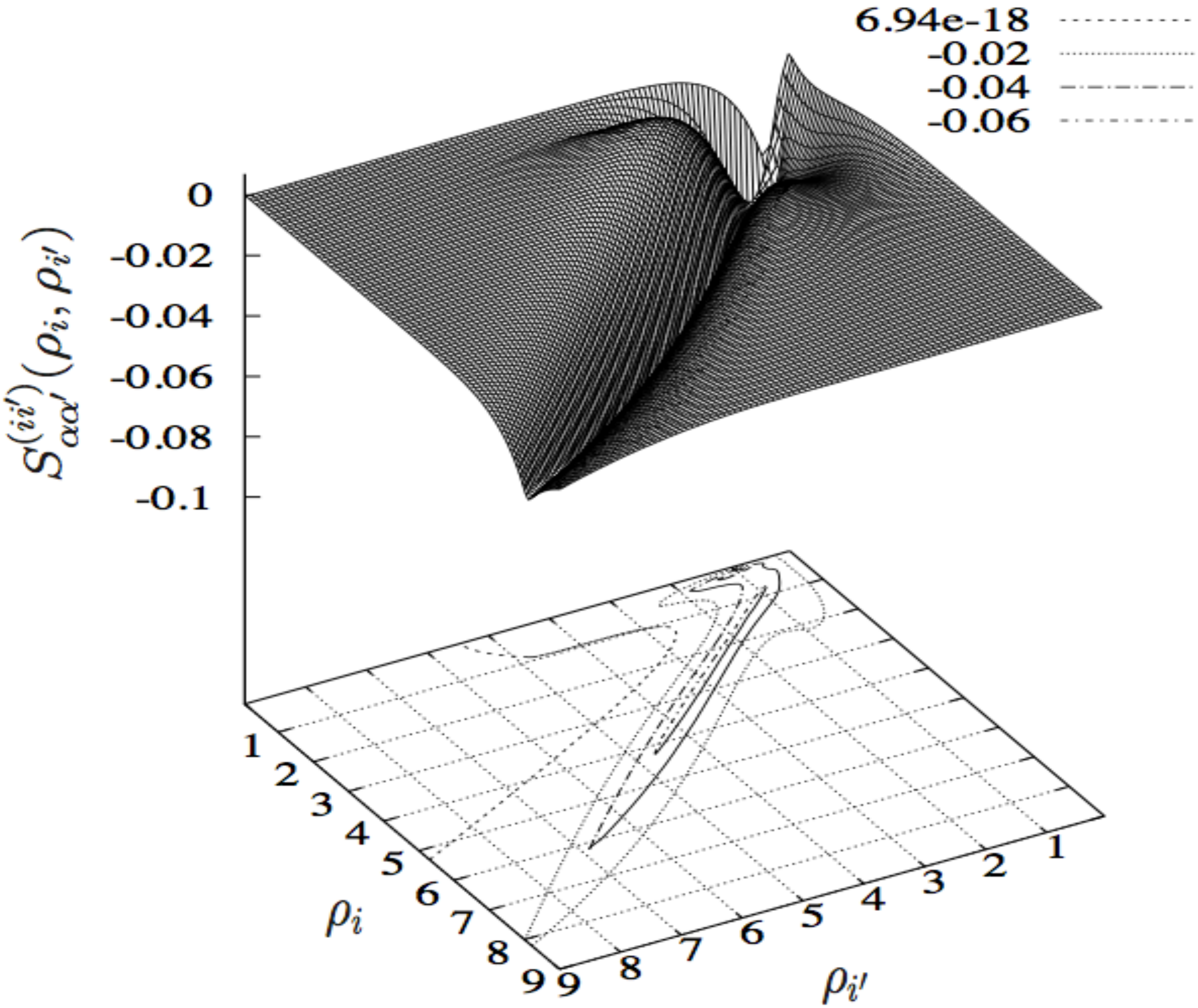

FIG. 5. The angular integral $S^{ii'}_{\alpha\alpha'}(\rho_i, \rho_{i'})$, Eq. (40), in the input channel $\overline{\mathrm{p}} + (\mu^+\mu^-)$ when α =1s and α' =2p.

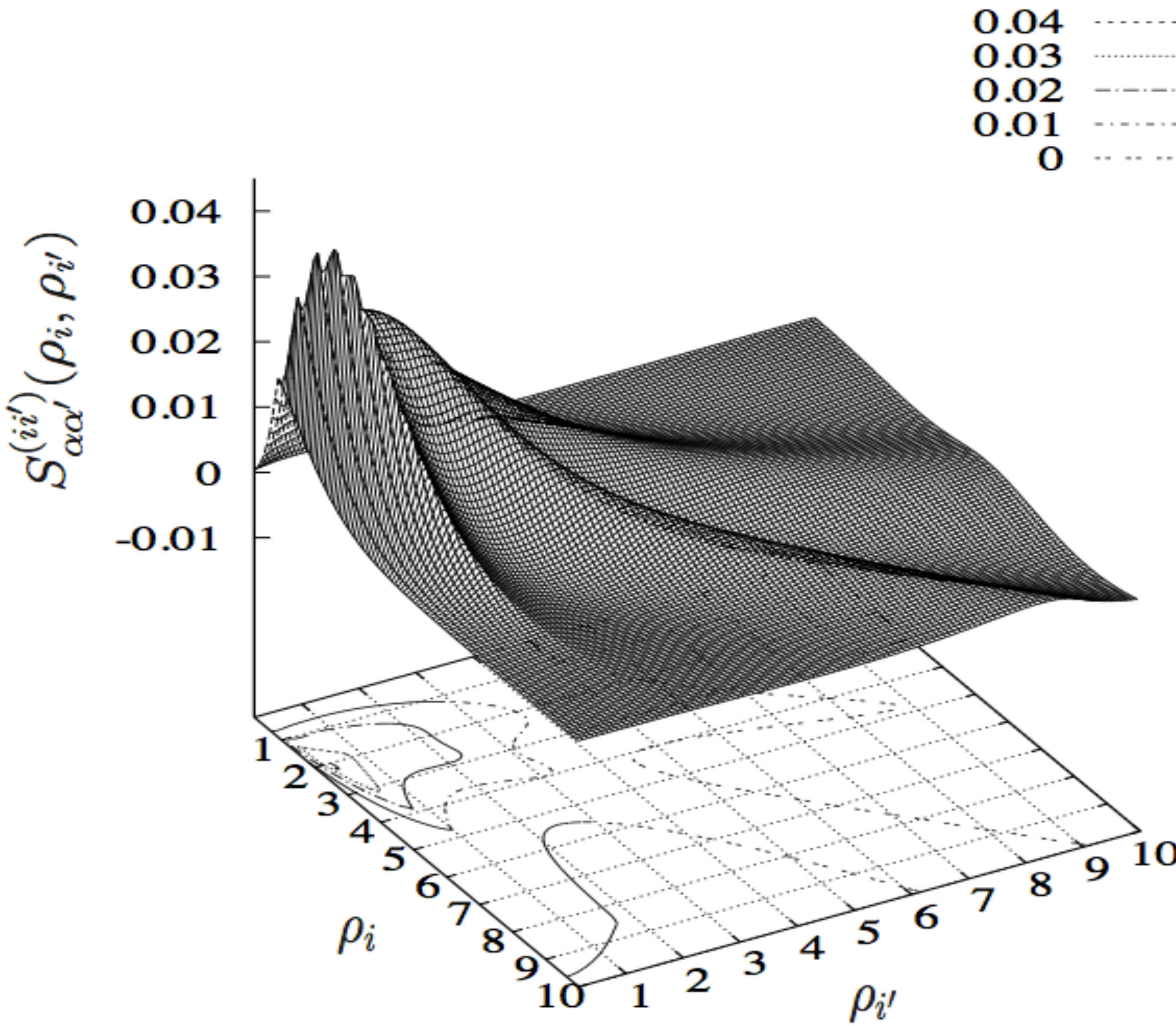

FIG. 6. The angular integral $S^{ii'}_{\alpha\alpha'}(\rho_i, \rho_{i'})$, Eq. (40), in the input channel $\overline{\mathrm{p}} + (\mu^+\mu^-)$ when α =2p and α' =2p.

RESULTS (arXiv:1304.2434v2)

1). $t^{+} + (d\mu)_{1s} \rightarrow (t\mu)_{1s} + d^{+}$

2). $t^{+} + (p\mu)_{1s} \rightarrow (t\mu)_{1s} + p^{+}$

3). $d^{+} + (p\mu)_{1s} \rightarrow (d\mu)_{1s} + p^{+}$

4). pbar + Ps $\rightarrow \bar{H} + e^{-}$

5). pbar + $(Ps)_{\mu} \rightarrow \bar{H}_{\mu} + \mu^{-}$

HERE: $t^{+} = {}^{3}\mathbf{H}^{+}$; $d^{+} = {}^{2}\mathbf{H}^{+}$; $p^{+} = {}^{1}\mathbf{H}^{+}$; μ^{-}

pbar=p^{-} ; Ps = $(\mathbf{e}^{+}\,\mathbf{e}^{-})$; $(Ps)_{\mu}=(\boldsymbol{\mu}^{+}\,\boldsymbol{\mu}^{-})$.

$$t^+ + (d\mu)_{1s} \rightarrow (t\mu)_{1s} + d^+$$

- Rearrangement scattering at low energies;
- Only total angular momentum L=0, 1s+2s +2p in the expansion functions;
- Muon transfer reaction cross sections has been computed; AND…
- Low energy muon transfer rate:

$$\lambda = \sigma\, v\, N = \text{const}\,!$$

0.1000000E-02	0.1977003E-02	0.4294772E+00	0.7217010E-04	0.1519791E-18	0.7385885E+02	0.2540629E+09	0.9938121E+00
0.5000000E-02	0.4420714E-02	0.4294951E+00	0.1611157E-03	0.6785697E-19	0.3297715E+02	0.2536512E+09	0.9938271E+00
0.1000000E-01	0.6251833E-02	0.4295174E+00	0.2274107E-03	0.4788919E-19	0.2327320E+02	0.2531599E+09	0.9938458E+00
0.5000000E-01	0.1397952E-01	0.4296961E+00	0.5009274E-03	0.2109752E-19	0.1025298E+02	0.2493870E+09	0.9939957E+00
0.1000000E+00	0.1977003E-01	0.4299195E+00	0.6954165E-03	0.1464440E-19	0.7116890E+01	0.2448099E+09	0.9941834E+00
0.5000000E+00	0.4420714E-01	0.4317018E+00	0.1338879E-02	0.5638946E-20	0.2740417E+01	0.2107853E+09	0.9956979E+00
0.1000000E+01	0.6251833E-01	0.4339195E+00	0.1547403E-02	0.3258592E-20	0.1583611E+01	0.1722612E+09	0.9976308E+00
0.2000000E+01	0.8841427E-01	0.4383211E+00	0.1272741E-02	0.1340098E-20	0.6512614E+00	0.1001865E+09	0.1001733E+01
0.3000000E+01	0.1082849E+00	0.4426790E+00	0.4467490E-03	0.3135949E-21	0.1524009E+00	0.2871355E+08	0.1007154E+01
0.5000000E+01	0.1397952E+00	0.4512685E+00	0.8914081E-02	0.3754337E-20	0.1824533E+01	0.4437880E+09	0.1010586E+01
0.6000000E+01	0.1531380E+00	0.4555025E+00	0.1169951E-01	0.4106229E-20	0.1995546E+01	0.5317116E+09	0.1015013E+01
0.7000000E+01	0.1654080E+00	0.4596975E+00	0.9675798E-02	0.2910820E-20	0.1414601E+01	0.4071194E+09	0.1019120E+01
0.8000000E+01	0.1768285E+00	0.4638546E+00	0.8265681E-02	0.2175782E-20	0.1057387E+01	0.3253251E+09	0.1023143E+01
0.9000000E+01	0.1875550E+00	0.4679748E+00	0.7317177E-02	0.1712094E-20	0.8320440E+00	0.2715228E+09	0.1027135E+01
0.1000000E+02	0.1977003E+00	0.4720590E+00	0.6565834E-02	0.1382664E-20	0.6719472E+00	0.2311394E+09	0.1031112E+01
0.2000000E+02	0.2795905E+00	0.5111091E+00	0.6597714E-02	0.6946885E-21	0.3376049E+00	0.1642338E+09	0.9695740E+00
0.3000000E+02	0.3424270E+00	0.5473804E+00	0.2647358E-01	0.1858310E-20	0.9031019E+00	0.5380667E+09	0.9748105E+00
0.3500000E+02	0.3698634E+00	0.5646431E+00	0.4854933E-02	0.2921069E-21	0.1419582E+00	0.9135518E+08	0.9800934E+00
0.4000000E+02	0.3954006E+00	0.5813933E+00	0.2263657E-02	0.1191728E-21	0.5791565E-01	0.3984416E+08	0.9870931E+00
0.5000000E+02	0.4420714E+00	0.6135235E+00	0.7838095E-02	0.3301164E-21	0.1604301E+00	0.1233984E+09	0.1003287E+01
0.6000000E+02	0.4842649E+00	0.6440527E+00	0.2420615E-01	0.8495736E-21	0.4128760E+00	0.3478836E+09	0.1021792E+01
0.7000000E+02	0.5230659E+00	0.6731989E+00	0.1126654E-02	0.3389372E-22	0.1647168E-01	0.1499083E+08	0.1041832E+01
0.8000000E+02	0.5591809E+00	0.7011345E+00	0.2798618E-02	0.7366823E-22	0.3580131E-01	0.3483233E+08	0.1061578E+01
0.9000000E+02	0.5931010E+00	0.7279989E+00	0.2144936E-02	0.5018783E-22	0.2439029E-01	0.2516964E+08	0.1081514E+01

Muon transfer: $\lambda = \sigma\, v\, N$

$\lambda = 2.6 \times 10^{-8}\ s^{-1}$

This work, FH equations (1s+2s+2p and the total orbital momentum only L=0: at low energies this is good).

$\lambda = 2.8 \times 10^{-8}\ s^{-1}$

(Kino, Kamimura, Hyper. Int. **82**, 45 (1993)).

$\lambda = 2.8 \times 10^{-8}\ s^{-1}$ & $3.5 \times 10^{-8}\ s^{-1}$

(Breunlich et al. (Experiment) in PRL **58**, 329 (1987)).

$t^+ + (p\mu)_{1s} \rightarrow (t\mu)_{1s} + p^+$

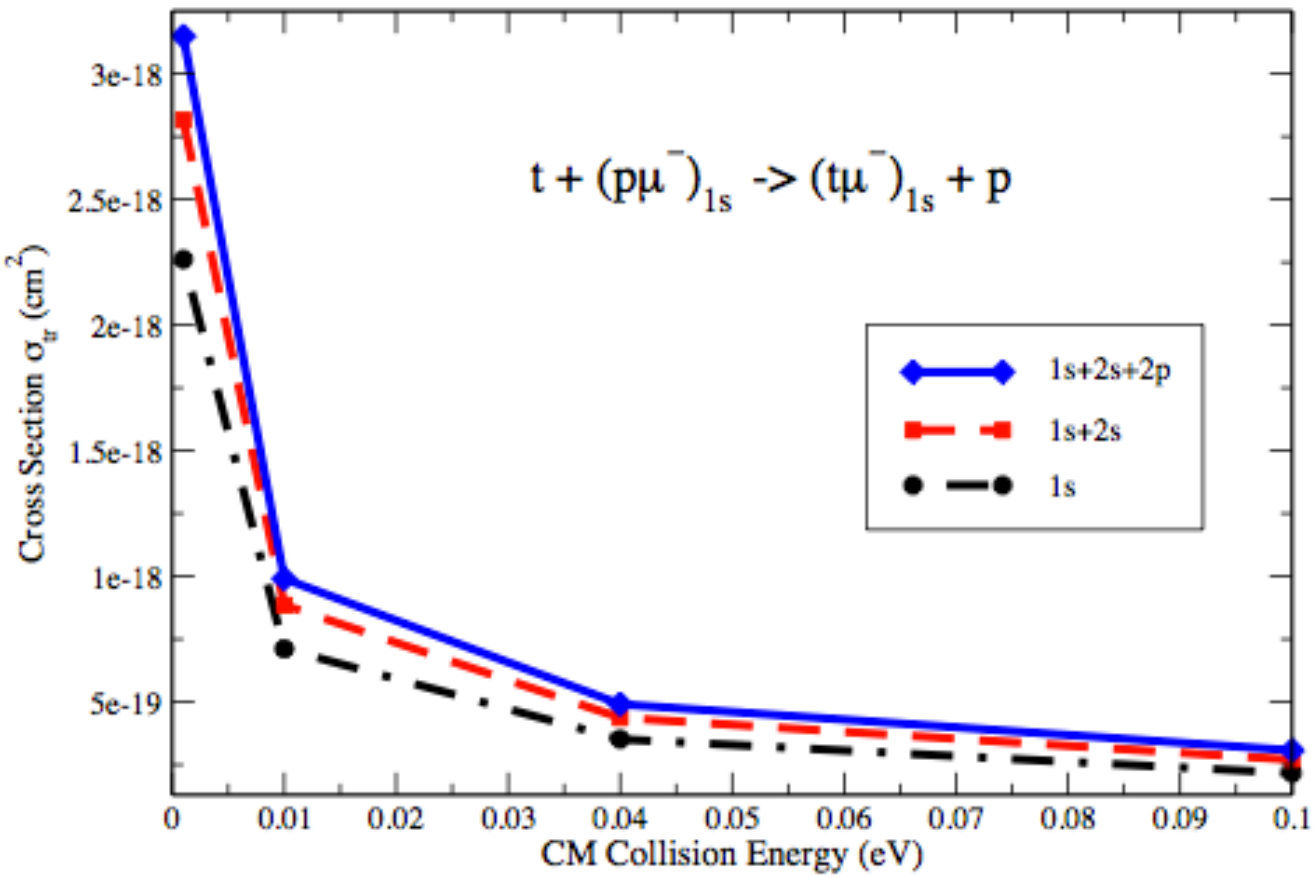

$d^+ + (p\mu)_{1s} \rightarrow (d\mu)_{1s} + p^+$

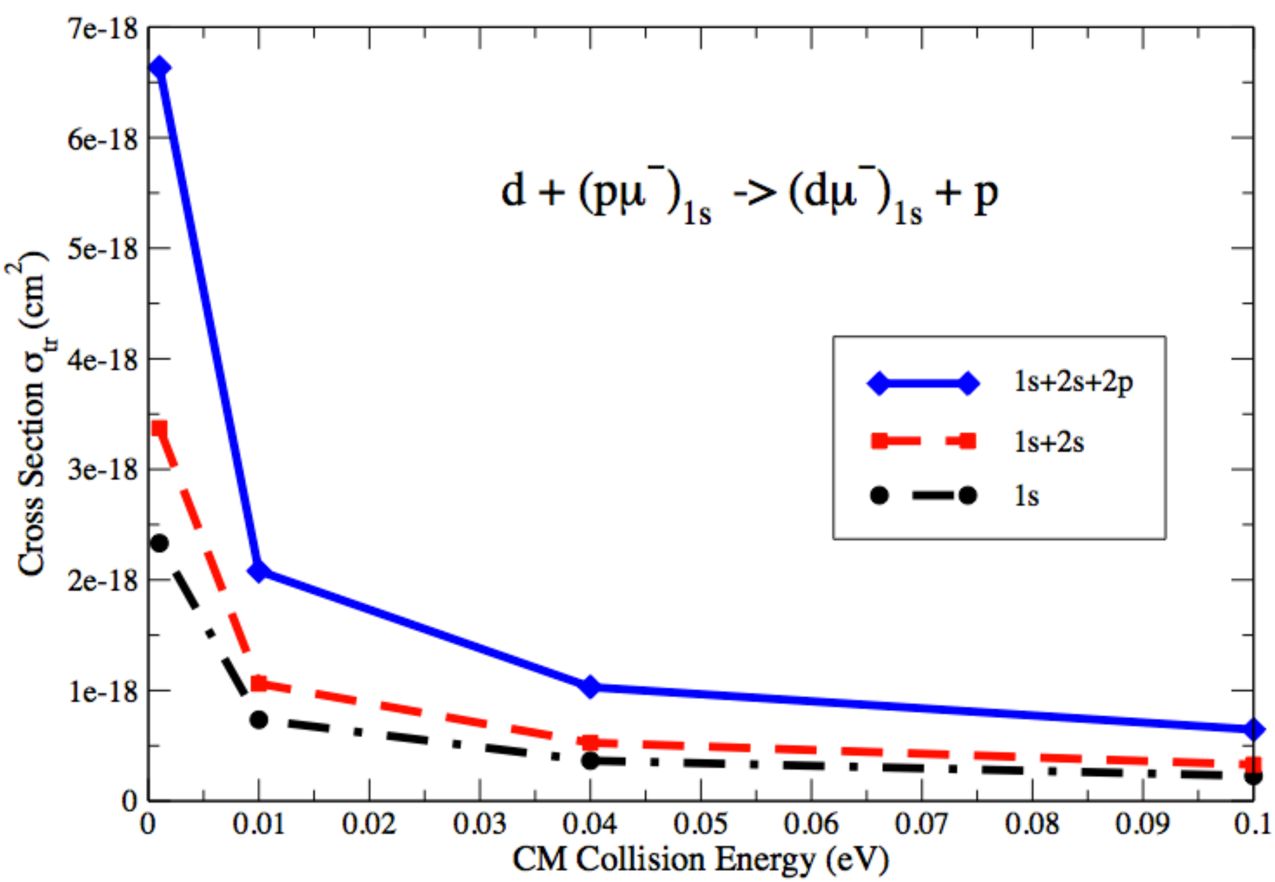

TABLE I. Cross sections σ_{tr} and rates λ_{tr}, Eq. (41), for μ^- transfer reactions from a light hydrogen isotope to a heavier hydrogen isotope at low collision energies together with other theoretical results and experimental data. The result for unitarity ratio K_{21}/K_{12}, Eq. (37), are also presented for t+$(\mathrm{d}\mu)_{1s}$.

Energy, eV	Method	t+$(\mathrm{d}\mu)_{1s} \to (\mathrm{t}\mu)_{1s}$+d			t+$(\mathrm{p}\mu)_{1s} \to (\mathrm{t}\mu)_{1s}$+p		d+$(\mathrm{p}\mu)_{1s} \to (\mathrm{d}\mu)_{1s}$+p	
		$\sigma_{tr}/10^{-20}$, cm^2	$\lambda_{tr}/10^8$, s^{-1}	K_{21}/K_{12}	$\sigma_{tr}/10^{-20}$, cm^2	$\lambda_{tr}/10^8$, s^{-1}	$\sigma_{tr}/10^{-20}$, cm^2	$\lambda_{tr}/10^8$, s^{-1}
0.001	FH-type Eqs.:	15.4	2.6	0.99	315.0	65.1	663.4	146.0
	[36]	15.8	2.7		384.4	80.0	828.7	170.0
	[37]	21.5	3.5		265.0	55.0	650.0	140.0
	[38]	18.0	2.8					
	[39]	14.2						
	Experiments:		2.8±0.5[58]			58.6±10[55]		84±13[54]
			2.8±0.3[57]					143±13[53]
			2.9±0.4[56]					95±34[52]
0.01	FH-type Eqs.:	4.84	2.6	0.99	99.1	64.7	208.1	144.8
	[36]	5.64			128.0		283.7	
	[37]	4.8			60.0		140.0	
	[38]	5.0						
	[39]	4.44						
0.04	FH-type Eqs.:	2.37	2.5	0.99	49.1	64.2	103.1	143.4
	[36]	2.94			63.6		140.7	
	[37]	3.1			40.0		91.0	
	[38]	2.5						
0.1	FH-type Eqs.:	1.42	2.4	0.99	30.7	63.5	64.6	142.1
	[36]	2.0			39.9		87.4	
	[39]	1.35						

pbar + Ps → H̄ + e⁻

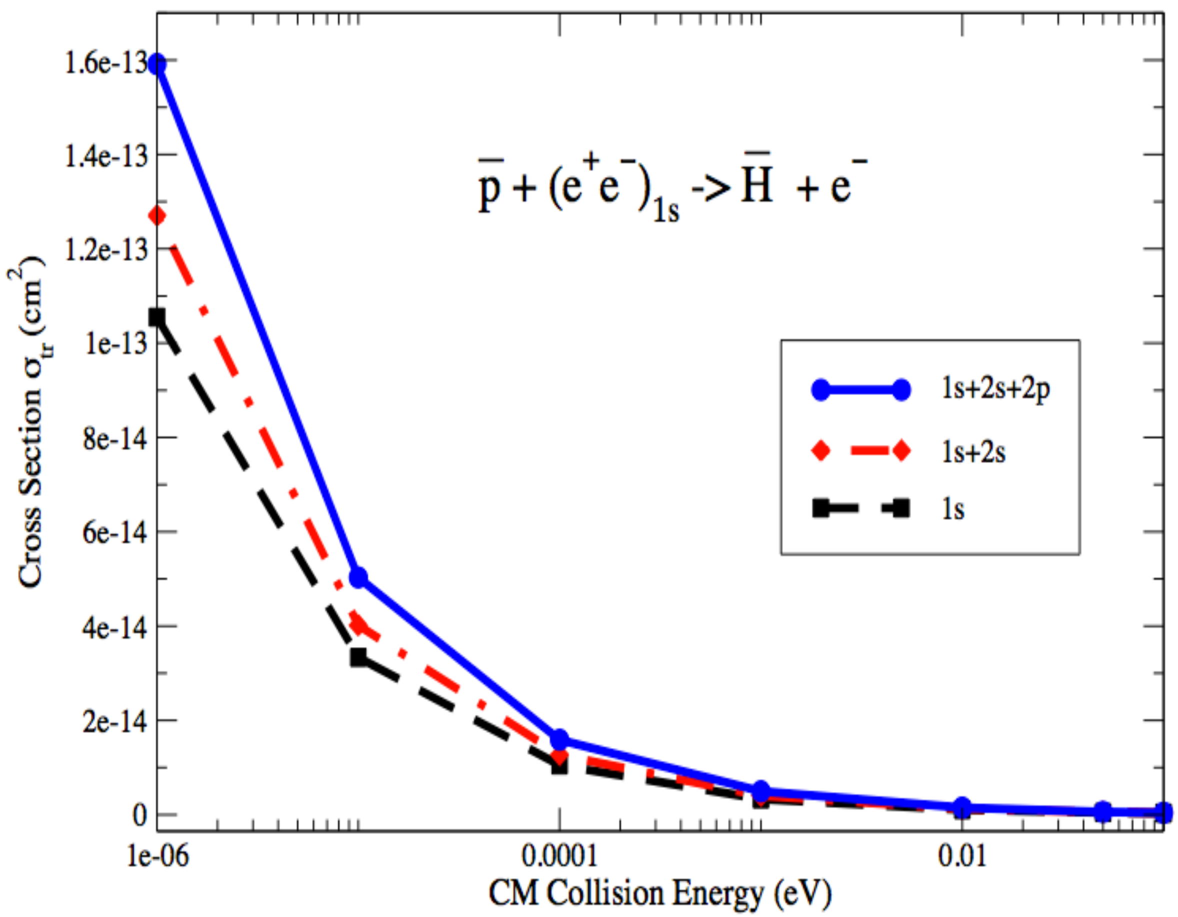

$\bar{p} + (e^+e^-)_{1s} \rightarrow \bar{H} + e^-$
1s+2s+2p
1s+2s
1s
Cross Section σ_{tr} (cm^2)
1.6e-13
1.4e-13
1.2e-13
1e-13
8e-14
6e-14
4e-14
2e-14
0
1e-06
0.0001
0.01
CM Collision Energy (eV)

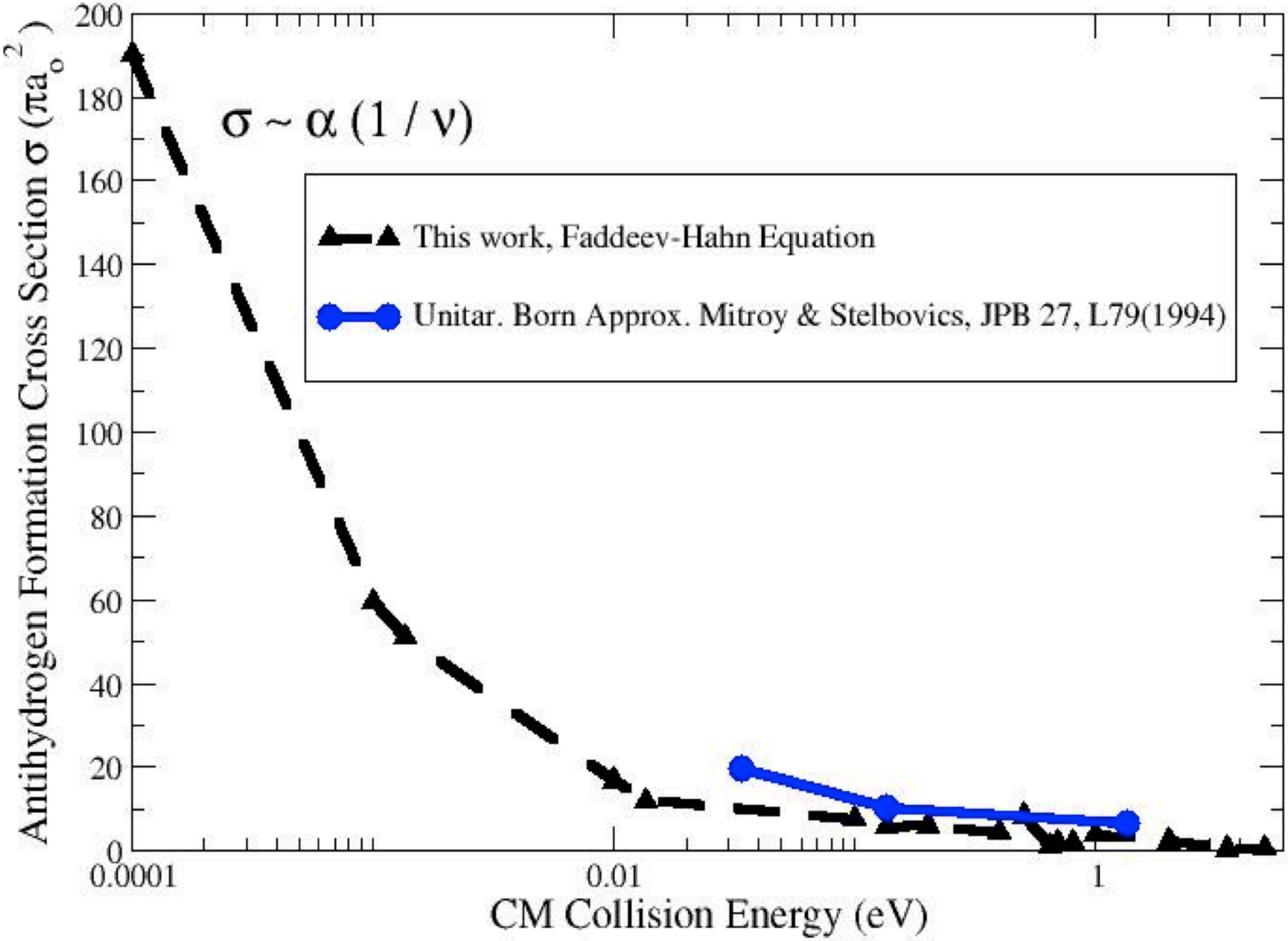

Antihydrogen Formation Cross Section σ (πa_o^2)
σ ~ α (1 / ν)
This work, Faddeev-Hahn Equation
Unitar. Born Approx. Mitroy & Stelbovics, JPB 27, L79(1994)
200
180
160
140
120
100
80
60
40
20
0
0.0001
0.01
1
CM Collision Energy (eV)

TABLE II. The total cross sections $\sigma_{\overline{\rm H}}$ and $\sigma_{\overline{\rm H}_\mu}$ for the reactions (1) and (2) respectively. The product of these cross sections and the corresponding center-of-mass velocities $v_{c.m.}$ between $\overline{\rm p}$ and Ps=(e^+e^-), i.e. $\sigma_{\overline{\rm H}} v_{c.m.}$ and between $\overline{\rm p}$ and the true muonium atom $\text{Ps}_\mu = (\mu^+\mu^-)$, i.e. $\sigma_{\overline{\rm H}_\mu} v_{c.m.}$ are presented.

	$\overline{\rm p} + (e^+e^-)_{1s} \to \overline{\rm H} + e^-$		$\overline{\rm p} + (\mu^+\mu^-)_{1s} \to \overline{\rm H}_\mu + \mu^-$	
E, eV	$\sigma_{\overline{\rm H}}$, cm^2	$\sigma_{\overline{\rm H}} v_{c.m.}$, cm^3/s	$\sigma_{\overline{\rm H}_\mu}$, cm^2	$\sigma_{\overline{\rm H}_\mu} v_{c.m.}$, cm^3/s
1.0e-06	0.16e-12	0.67e-08		
1.0e-05	0.50e-13	0.67e-08		
1.0e-04	0.16e-13	0.67e-08	0.18e-16	0.60e-12
1.0e-03	0.50e-14	0.66e-08	0.58e-17	0.60e-12
1.0e-02	0.15e-14	0.63e-08	0.18e-17	0.59e-12
5.0e-02	0.60e-15	0.56e-08	0.82e-18	0.59e-12
1.0e-01	0.42e-15	0.55e-08	0.58e-18	0.59e-12
5.0e-01			0.27e-18	0.62e-12
1.0e-00			0.23e-18	0.73e-12

Ħ PRODUCTION RATE

- **Now one can compute the rate of the Ħ - atom production:**

- **LEAR facility @ CERN:**

$$R = \sigma_{\bar{H}}\, n\, d\, I$$

Here:

n - the density of Ps atoms,

d - the linear dimension,

of the interaction region,

& **I** - intensity of the Ps atom beam.

$\bar{p} + (\mu^+\mu)^- \rightarrow \bar{H}_\mu + \mu^-$

- Here are new results for the title 3-particle reaction.
- Computation is done for low and very low energies: from 1 eV down to 10^{-4} eV.
- Very stable results for the rearrangement scattering cross sections **with good unitarity numbers**, i.e. $K_{12} / K_{21} \sim 1.0$.
- Only **1s**, **1s+2s and 1s+2s+2p** modified CC (close-coupling) approximation has been applied.

pbar + $(Ps)_\mu$ → $\bar{H}_\mu + \mu^-$

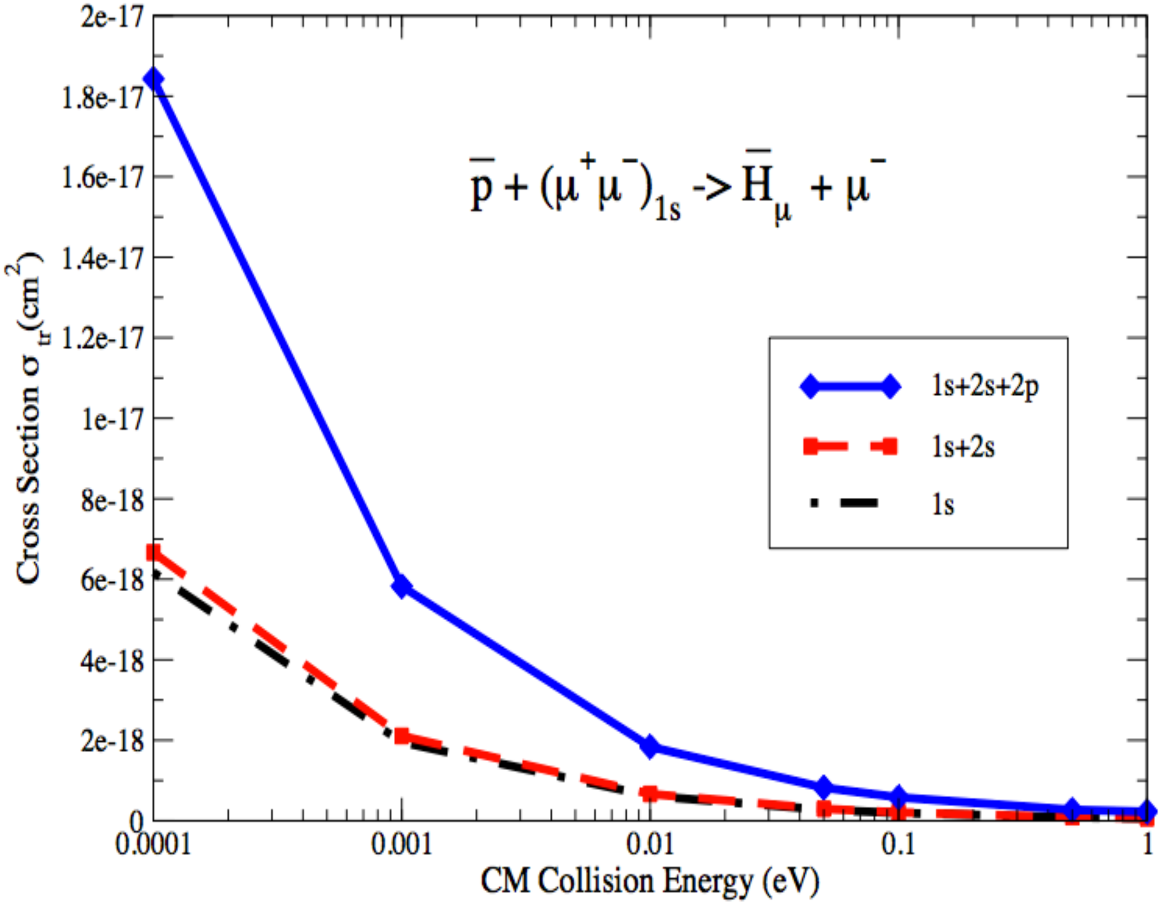

CONCLUSION

1. The antihydrogen (Ħ, $Ħ_μ$) formation cross sections have been computed from 3-charge-particle collisions at low and very low kinetic energies.

2. Test 3-body systems (muon transfer) have also been computed.

3. Normal and muonic antihydrogen formation thermal rates are computed at low and very low temperatures: $T \sim 10^{-1}$ K. This is important in view of possible near future, very low energy antiproton beams at CERN!

4. Later, it may be useful to increase the expansion basis: **1s +2s+2p+3s+3p+3d+…**

5. Consider higher values of the total 3-body angular momentum L, i.e. **L > 0** (currently L=0).

ADDITION

- If time permits: about Takayanagi's modified wave number approximation in order to take into account and compute contributions of higher values of the total angular momentum L.

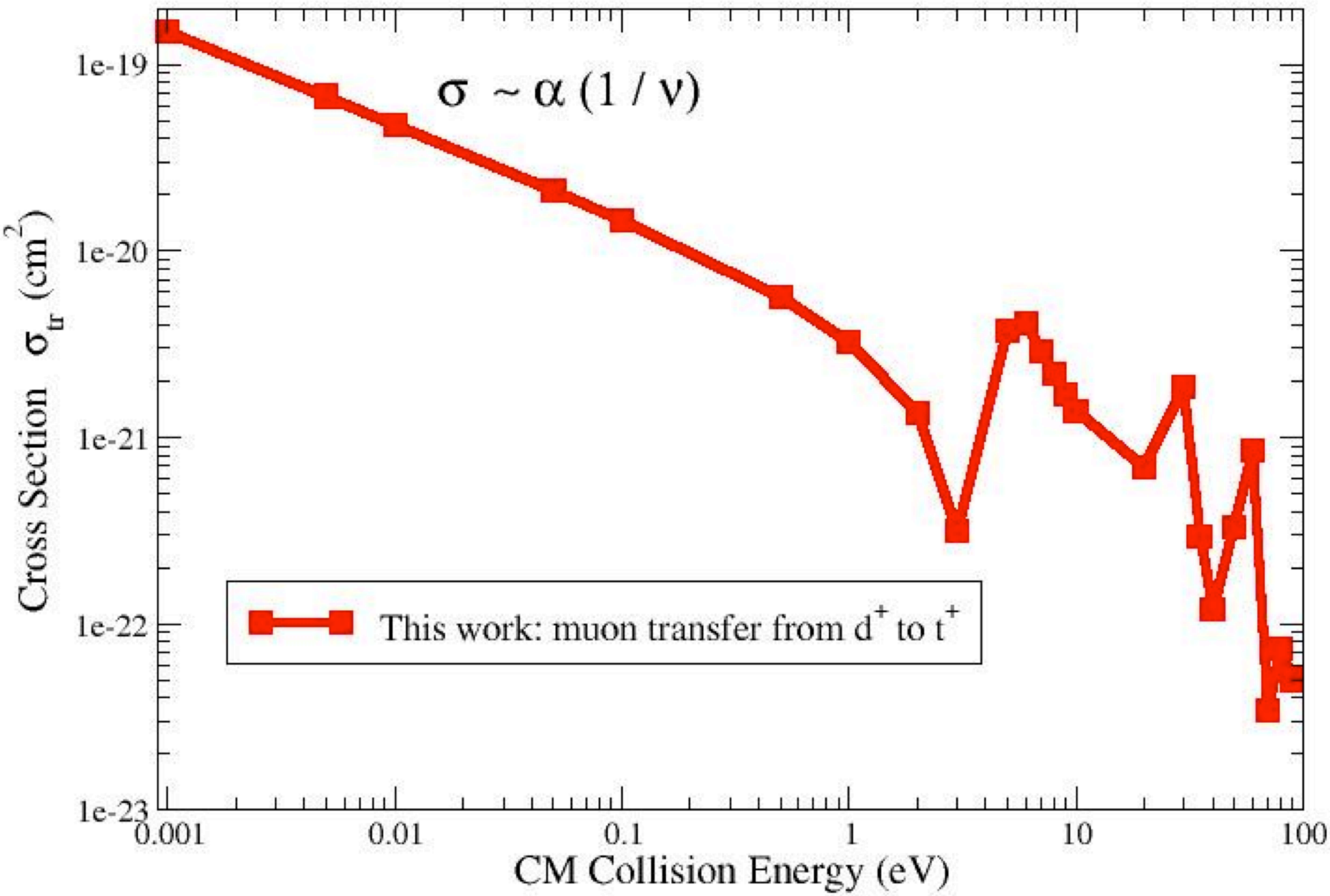

σ ~ α (1 / ν)
Cross Section σ_tr (cm^2)
1e-19
1e-20
1e-21
1e-22
1e-23
0.001
0.01
0.1
1
10
100
CM Collision Energy (eV)
This work: muon transfer from d+ to t+

The Takayanagi Method: Modified Wave Number Approximation: **MWNA** (1950-60's)"

- In order to take into account an important contribution from the higher values of the total angular momentum L, i.e. L > 0. *Important:* below "J" and our "L" are the same 3-body angular momenta, i.e. J=L!
- This method (MWNA) was originally introduced in some molecular physics applications such as H_2+H_2: **K. Takayanagi, Adv. At. Mol. Phys. pp. 149-193 (1965).**
- Later this approach became a prototype for a very successful and widely used in computational quantum chemistry: The Famous ***J-shifting Approximation*.**

$$\sigma(nl \to n'l') = \frac{\pi}{k_\alpha^2} \sum_J (2J+1) P(J; k'_\beta, k_\alpha)$$

$$\boxed{P(J; k'_\beta, k_\alpha) \approx P(J=0; \tilde{k}'_\beta, \tilde{k}_\alpha)}$$

$$(\tilde{k}'_\beta)^2 = (k_\beta)^2 - \frac{J(J+1)}{R_c^2}$$

$$(\tilde{k}_\alpha)^2 = (k_\alpha)^2 - \frac{J(J+1)}{R_c^2}$$

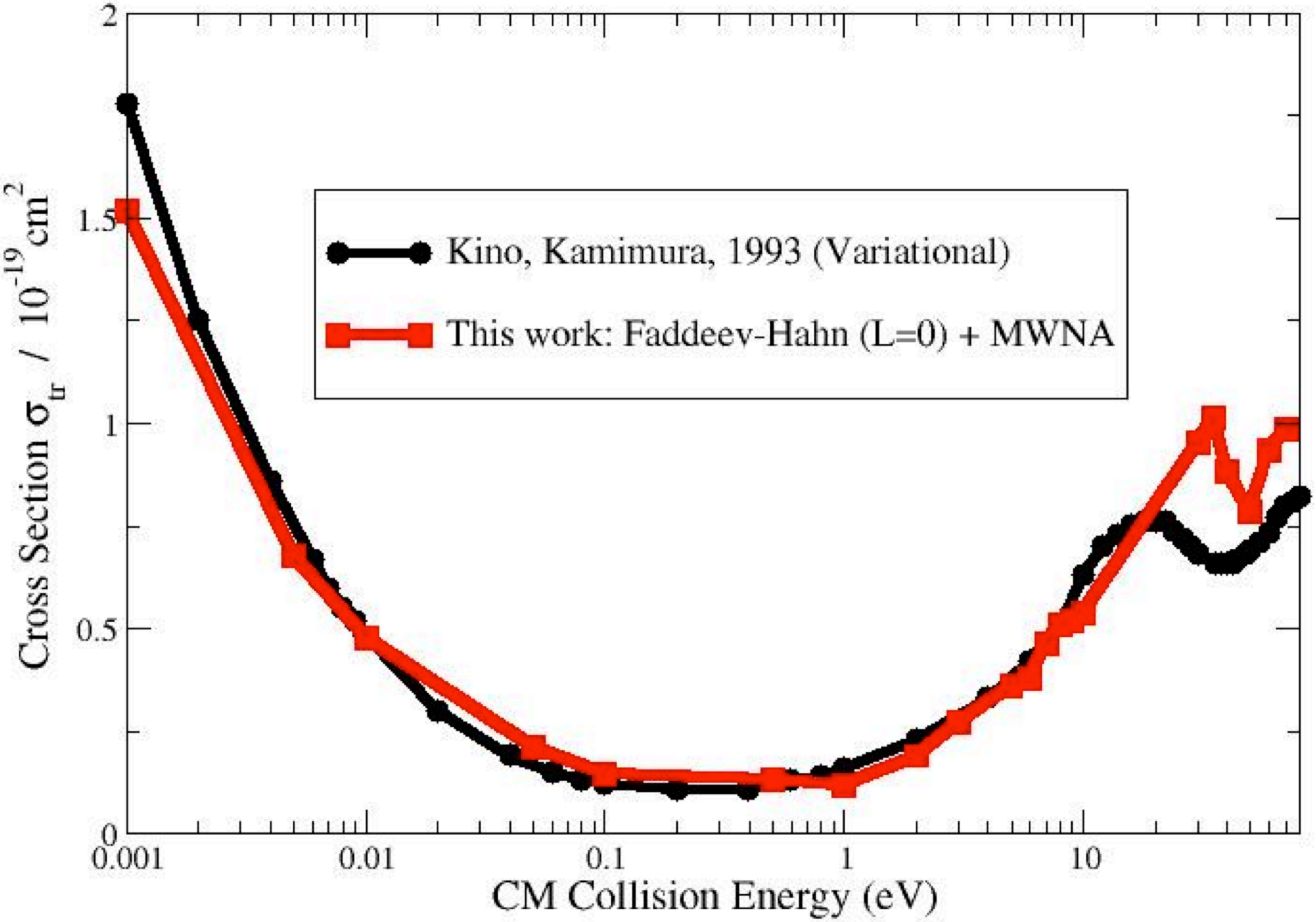

Kino, Kamimura, 1993 (Variational)
This work: Faddeev-Hahn (L=0) + MWNA
Cross Section σ_{tr} / 10^{-19} cm^2
CM Collision Energy (eV)
0
0.5
1
1.5
2
0.001
0.01
0.1
1
10